NASA(NGR)33-010-189 No.5

ELASTIC MODULI OF PRECOMPRESSED PYROPHYLLITE USED IN ULTRAHIGH PRESSURE RESEARCH

by

Wolfgang Sachse

Department of Theoretical and Applied Mechanics

Arthur L. Ruoff

Department of Materials Science and Engineering

Cornell University

Ithaca, N. Y. 14853

December 1974

Report #2366

Issued by

The Materials Science Center

ELASTIC MODULI OF PRECOMPRESSED PYROPHYLLITE USED IN ULTRAHIGH PRESSURE RESEARCH

Wolfgang Sachse
Department of Theoretical and Applied Mechanics

Arthur L. Ruoff
Department of Materials Science and Engineering

Cornell University
Ithaca, N. Y. 14853

ABSTRACT

Chao and Ruoff [*] have shown previously that by precompressing pyrophyllite prior to its use in high-pressure applications, one obtains a material which has a uniform density and uniform mechanical properties. We have recently studied the propagation of ultrasonic pulses in pyrophyllite specimens to investigate the effect of specimen precompression on the measured elastic moduli. Measurements were made at room pressure and, for the precompressed specimens, to pressures of 3 kbar.

We find pyrophyllite to be elastically anisotropic, apparently the result of the fabric present in our material. The room pressure adiabatic bulk modulus as measured on specimens made of isostatically compacted powdered pyrophyllite was determined to be 96.1 kbar. We found the wave speeds of ultrasonic pulses in pyrophyllite to decrease with increasing specimen precompression. A limiting value of precompression was found, above which no further decrease in wave speed is observed. For the shear wave speeds this occurs at 10 kbar while for the longitudinal wave at 25 kbar. In the limit, the shear waves propagate 20% slower than in the unprecompressed samples; for the longitudinal wave the

---

[*] C. C. Chao and A. L. Ruoff, Rev. Sci. Instr., 41, 720-721 (1970).

I. INTRODUCTION

The use of pyrophyllite as an anvil - supporting material and as a pressure-transmitting medium in a Drickamer-type pressure apparatus is well known [1] Chao and Ruoff [2] have shown that by precompressing the pyrophyllite prior to its use, one obtains a material having uniform density and exhibiting uniform mechanical properties. They showed that this results in an improved work hardening response of the tungsten carbide pistons in the Drickamer pressure apparatus. In a recent publication [3], Ruoff has noted that the flow stress of many solids varies linearly with pressure, the rate involving the first pressure derivative of the effective elastic modulus.

Although the characteristics and structure of pyrophyllite are well known [4-6], the authors have been unable to locate any publications concerning the elastic moduli of pyrophyllite or the pressure derivatives of these. Inasmuch as this precompressed material is expected to continue to find widespread application in ultrahigh pressure research, we studied the propagation of ultrasonic pulses in pyrophyllite specimens, precompressed varying amounts to pressures of 40 kbar, to determine their elastic moduli at atmospheric pressure.

Motivated by the aforementioned pressure-dependent flow-stress concept, we also measured the room-temperature pressure derivatives of the moduli in a range to 3 kbar above room pressure using 40 kbar precompressed pyrophyllite samples.

II. EXPERIMENTAL

a) Specimens

Three types of pyrophyllite specimens having differing precompression histories were prepared. One series consisted of specimens as received, another consisted of specimens all precompressed to 40 kbar and a third consisted of a series of specimens each precompressed a varying amount which

difference is 30%.

The change in bulk modulus resulting from increasing pressure shows a behavior which can be approximated by a bi-linear curve with decreasing slope, the discontinuity occurring between 1.6 and 1.8 kbar. In the second portion of the curve, the bulk modulus derivative is determined to be 22.1. We believe that this value indicates the presence of voids which are closing under pressure. A regression analysis of the data shows that a $P^{1/2}$ equation appears to give the best fit. The resulting empirical law for the bulk modulus derivative at pressure P becomes:

$$\frac{dB}{dP} = \left[\frac{C_{L_o}}{(0.251P-0.147)^{1/2}} - \frac{C_{S_o}}{(2.76P-2.56)^{1/2}} \right] \times 10^{-1}$$

where P is in kbars and in the present measurements C_{L_o}, the longitudinal modulus, is 204 kbar and C_{S_o}, the average shear modulus, is 113 kbar.

ranged from 5 kbar to 40 kbar.

All specimens were cut from one portion of a large block of grade A pyrophyllite purchased from the Maryland Lava Company. The specimens were fine-grained (smaller than 0.5mm) pyrophyllite having an observable fabric comprised of an alignment of the pyrophyllite grains and wispy greyish areas within the pyrophyllite. Visible under polarized light are several rectangular areas which may be pseudo-morphs after pyroxene because they exhibit mass extinction. Present also are small regions having limonitic stains, probably from the alteration of minute grains of pyrite, as well as spots of hematite coming from minute grains of magnetite. A micrograph of a typical section is shown in Figure 1.

The specimens comprising each of the three series listed above were cut sequentially from the length of the original section. The dimensions of all the specimen discs were 2.233 ± 0.003 cm in diameter and 0.528 ± .003 cm in thickness. The dimensions of each specimen were measured with a Vankeuren light-wave micrometer having a resolution of $\pm$ 1.3 x 10^{-5} cm. The faces of the specimens were parallel to $\pm$ 5 x 10^{-5} cm.

b) Density Determination

Most density determinations were made from specimen weight and dimensional measurements, but some were checked with a gravimetric method.

Because pyrophyllite is so porous, we coated the specimen with a thin, water-proofing coating (Krylon), which, in all cases, represented less than 0.05% of the specimen's weight when dry. We found that the amount of water absorption was limited to less than 0.17% of the specimen's weight after a five minute immersion in water containing a wetting agent. In all cases, the uncertainty in the density determination was less than 1%.

c) Ultrasonic Measurements

The velocities of pulses of ultrasonic longitudinal and shear waves were

measured using the pulse-echo technique. The radio-frequency pulse was generated and received by a (Matec Model 6600) r.f. pulse generator and receiver. Coaxially plated, 0.127 cm-dia., 2MHZ X - cut and AC - cut quartz transducers were used to generate longitudinal and shear wave pulses, respectively. The bond was sodium salicylitate (salol). The display oscilloscope was used to make transit-time determinations with an accuracy of 1 to 2%. Higher accuracy measurements were made with the echo-overlap technique [7]. Details of the system used for the present measurements have been described previously [8]. In this method, the overlap of any two echoes is achieved visually on the viewing oscilloscope by proper triggering of the oscilloscope and pulse generator. The echo-overlapping procedure was repeated ten times from which an average transit time $\bar{\tau}$ and its standard deviation $\pm \Delta\tau$ were computed. Absolute accuracy of the transit-time determination in the measurements reported here is better than 1 part in 10^4, while changes in pulse transit-time are accurate to 1 part in 10^6. The room pressure adiabatic longitudinal and shear moduli denoted by C_L^S and C_S^S respectively were evaluated using Equation (1)

$$C_o^S \pm \Delta C_o^S = \rho_o \left(\frac{2\ell_o}{\bar{\tau}_o}\right)^2 \left[1 \pm \left(\frac{\Delta\rho_o}{\rho_o} + \frac{2\Delta\ell_o}{\ell_o} + \frac{2\Delta\tau_o}{\bar{\tau}_o}\right)\right] \tag{1}$$

Here $\Delta\ell_o$ and $\Delta\rho_o$ represent respectively the uncertainties in ℓ_o the initial wave propagation distance and ρ_o the initial specimen density. In an isotropic solid, C_L^S corresponds to $\lambda + 2\mu$ and C_S^S to μ, where λ is the Lamé parameter and μ is the shear modulus.

The adiabatic bulk modulus B^S and Young's modulus E^S are given by the equations

$$B^S = C_L^S - 4/3\ C_S^S \tag{2}$$

and

$$E^S = 3C_S^S B^S / (C_L^S - C_S^S) \tag{3}$$

Only changes in the pulse transit-time were measured as a function of

applied hydrostatic pressure. The corresponding change of elastic modulus is then determined when the pressure-dependent specimen dimensional changes are taken into consideration. Determination of this length correction can be made if the isothermal bulk modulus B^T is known. It is related directly to the adiabatic bulk modulus by the equation

$$B^S/B^T = 1 + \frac{\beta^2 B^S T}{\rho c_P} \equiv 1 + \Delta_o \tag{4}$$

The correction term Δ_o contains β which represents the volume coefficient of thermal expansion ($= 3\alpha$)($9.9 \times 10^{-6}\ ^oK^{-1}$) [9]; B^S is the adiabatic bulk modulus (96.1 kbar) [Appendix B]; T is the absolute temperature (300°K); ρ_o, the density (2.738 g/cm^3) and c_p, which is the specific heat at constant pressure (0.22 cal/g^{o}K) [10]. Using these, we find Δ_o to be 1.12×10^{-4}.

The length at pressure P is then determined approximately for small length changes from

$$\ell_o/\ell_o(P) = 1 + \int_0^P \frac{(1+\Delta_o)}{3B^S}\, dP \tag{5}$$

so that the change in modulus including the length correction is determined from transit-time measurements according to

$$\frac{C^S}{C_o^S} - 1 = \left[1 + \int_0^P \left(\frac{1+\Delta_o}{3B^S}\right) dP\right] \left(\frac{\bar{\tau}_o}{\bar{\tau}}\right)^2 - 1 \tag{6}$$

Here $\bar{\tau}_o$ and $\bar{\tau}$ represent the average round-trip time-intervals at atmospheric pressure and at pressure P , respectively. The uncertainty in this determination of the change of the apparent modulus is given for our cylindrical specimens of initial dimensions r_o , ℓ_o as

$$\pm 2\left(\frac{\tau_o}{\tau}\right)^2 \left[2\,\frac{\Delta r_o}{r_o} + \frac{\Delta \ell_o}{\ell_o} + \frac{\Delta \tau_o}{\bar{\tau}} + \frac{\Delta \tau}{\bar{\tau}}\right] \tag{7}$$

We measured the attenuation of ultrasonic pulses travelling in pyrophyllite to be quite high (15-18 db/cm). As the specimens were quite thin,

we found that 2MHZ pulses provided optimal material penetration and pulse definition so that accurate transit-time determinations could be made.

The pressure system, using helium as a pressure medium has been described in detail previously [11]. Pressure measurements were made with a manganin cell which had been calibrated against the new absolute pressure gauge system developed by Lincoln [12].

III. RESULTS

A. Room Pressure Measurements (No Precompression)

The average density of the pyrophyllite as determined from eight specimens which had not undergone precompression was 2.675 ± 0.003 g/cm^3. From measurements of the longitudinal and shear wave speeds as a function of specimen location in the original pyrophyllite block, we found the average velocity of the longitudinal wave in all eight specimens to be 0.370 ± 0.004 cm/μsec. In each specimen we measured two distinct shear waves whose particle displacements were perpendicular to each other. The fast shear wave propagated with speed 0.267 ± 0.003 cm/μsec while the slow shear wave propagated with speed 0.233 ± 0.003 cm/μsec. This indicates that the material is elastically anisotropic which is not surprising considering the pronounced fabric observed in the optical micrographs.

B. Room Pressure Measurements (After Precompression)

The average density of eight specimens which had been precompressed 40 kbar was 2.738 ± 0.008 g/cm^3. From the wave speed measurements we found the average longitudinal wave speed to be 0.273 ± 0.004 cm/μsec and, as in the"as received" specimens, we observed two distinct shear waves which were measured to be 0.215 ± 0.002 cm/μsec and 0.192 ± 0.002 cm/μsec.

The pyrophyllite specimens which were precompressed varying amounts showed a permanent change in volume (increase in density) dependent on the

precompression load, similar to the results previously reported by Chao and Ruoff [2]. Shown in Figure 2 is the relationship between the volume ratio V/V_o and the precompression pressure - here V_o and V are respectively the volume of the disc prior to and subsequent to the precompression. Also shown in Figure 2 is the change in ultrasonic wave speed in specimens precompressed differing amounts. The effect of precompression on a specimen is to decrease the measured longitudinal wave speed monotonically with increasing precompression. Precompression pressures in excess of 20-25 kbar were found to result in no additional decrease in the wave speed.

The intercept at zero precompression corresponds to that measured for the eight uncompressed samples, while the wave speed measured above 20-25 kbar agrees within 5% of that measured for all eight 40-kbar precompressed specimens. The shear wave measurements show a similar behavior except that a precompression pressure of 10 kbar is sufficient to achieve the same shear wave speed behavior as observed in the 40 kbar precompressed specimens.

These results, though contrary to empirical velocity - density relationships, c. f. Birch [13,14], are expected if structural changes result from the precompression of the pyrophyllite. A comparison of powder x-ray patterns of as received pyrophyllite and that which has been precompressed 40 kbar shows considerable line broadening of the latter, indicating that structural changes have, in fact, taken place.

We investigated, in detail, the densification of pyrophyllite as a result of applied hydrostatic pressure in the range to 5 kbar. The specimens were in the form of cylinders 1 cm long and 1 cm in diameter. To insure against any exchange of gas between the specimen and the pressure medium, the specimens were compressed with a wet-bag technique in a pressure system in which mineral oil was the pressure medium. The specimen was held under pressure for thirty minutes to insure thermal equilibrium. After removal from the pressure vessel,

the specimen was unbagged, its axial deformation measured, rebagged and returned to the pressure vessel for the next loading cycle. Calculation of the volume change was made from measurement of the axial deformation and the assumption that our fine-grained specimens densified isotropically. The results obtained from three specimens is shown in Figure 3. Also shown in this figure are the volume ratios of the specimen precompressed 5 kbar and that precompressed 10 kbar, which were shown previously in Figure 2.

We see that the change of volume appears to proceed in two stages, joining at approximately 1.8 kbar. These observations are similar to the predictions which Nelson [15] makes from consideration of a model describing the collapse of a single void in a plastically-deforming matrix. The first stage results from a non-linear stress-strain response of the elastically-deforming matrix while the second stage is predicted from consideration of the equilibrium between additional growth of the plastic zone of the matrix and collapse of the void contained in it.

C. Pyrophyllite Modulus Measurements as a Function of Pressure

Ultrasonic wave speed measurements could be made consistently to pressures of 3 kbar before the specimen-transducer bond failed. Measurements were made every 200 bars during pressurization and depressurization in 30 minute intervals to insure thermal equilibrium between the specimen and the pressure system.

The changes of the apparent longitudinal and (fast) shear moduli, defined previously by equation (7), resulting from hydrostatic pressure are shown in Figure 4. Both curves exhibit an initial, linear change with pressure which decreases significantly at pressures exceeding 1.6-1.8 kbar. The drawn-in straight-line segments result from a linear regression analysis of the data in each region, above and below 1.8 kbar.

The slopes of these lines are related directly to the first pressure

derivative of the elastic constant, being in fact,

$$\frac{1}{C_o}\frac{dC}{dP}$$

By assuming the shear modulus $\tilde{C}_S$ to be approximately equal to the average of the moduli specified by each of the two shear waves, we can evaluate the apparent Young's modulus E^S and the apparent adiabatic bulk modulus B^S for our specimens of pyrophyllite using equations (2) and (3). Our results are summarized in Table I. We see from Table I that the large change of modulus with pressure shown in Figure 4 results in an extraordinary large bulk modulus pressure derivative below 1.6 kbar. Above this pressure, that is, in the upper portions of the bi-linear curves, the derivative, though reduced, is still far greater than generally observed for most materials [16]. Bundy [17] determined B_o and B_o' from direct pressure vs. volume measurements of pyrophyllite in the range to 20 kbar and he found B_o to be 267.2 kbar and B_o' to be 20.2 kbar. The B_o^S measured ultrasonically in the present investigation is far lower than that determined quasi-statically by Bundy. However, the pressure derivative $B^{S'}$ measured in the range above 1.8 kbar is similar to that measured by Bundy.

We believe that the low initial bulk modulus and its large pressure derivative are the result of the presence of voids which are closing under pressure. It is possible that even the material which has been precompressed 40 kbar contains voids which open during the unloading of the precompression load. We attempted to coat a specimen with transducer attached using a silicone sealant (RTV) to prevent any possible exchange of gas between the specimen and the pressure medium. Unfortunately, the coating resulted in such a large increase in attenuation of the ultrasonic pulses which precluded all wave-speed measurements.

As an alternative, we used a regression analysis with the measured modulus

data to determine an analytic form for the change of modulus of the specimens resulting from the applied pressure. A linear, parabolic, general power and exponential least-square regression analysis was made to determine which gives the most accurate description (as measured by the correlation coefficient) of the experimental data. Figure 5 shows the results of this analysis applied to the data presented in Figure 4. The parabolic equation in pressure P gives the best description which becomes:

$$(C/C_o-1) = -\frac{\lambda_2}{2\lambda_1} + \left[P/\lambda_1 - \left(\frac{2\lambda_3-\lambda_2}{\lambda_1}\right)^2\right]^{1/2}$$

where P is the pressure in kbars, and

when $C = C_L$	when $C = C_S$
$\lambda_1 = 6.26$	$\lambda_1 = 1.23 \times 10^2$
$\lambda_2 = 1.01$	$\lambda_2 = -1.04 \times 10^1$
$\lambda_3 = 0.628$	$\lambda_3 = 1.15$

Using the above and equation (2) we can compute the adiabatic bulk modulus and its pressure derivative as a function of pressure P. We obtain for the latter

$$\frac{dB}{dP} = \frac{C_{L_o}}{(0.251P-0.147)^{1/2}} - \frac{C_{S_o}}{(2.76P-2.56)^{1/2}} \times 10^{-1}$$

This result is plotted to 50 kbar in Figure 6. It shows that the equation predicts the bulk modulus derivative to be less than 6.0 at pressures in excess of 30 kbar. We show for comparison the result which is obtained if the modulus change resulting from pressure is described by a general power law or a logarithmic law.

CONCLUSIONS

Our measurements clearly show pyrophyllite to be elastically anisotropic, apparently the result of the pronounced fabric present in our material. The

room pressure adiabatic bulk modulus as measured on an isostatically compacted specimen was determined to be 96.1 kbar. We found the wave speeds of ultrasonic pulses in pyrophyllite to decrease with increasing specimen precompression. A limiting value of precompression was found, above which no further decrease in wave speed is observed. For the shear wave speeds this occurs at 10 kbar while for the longitudinal wave at 25 kbar. In the limit, the shear waves propagate 20% slower than in the uncompressed samples; for the longitudinal wave the difference is 30%.

The change in modulus resulting from increasing pressure shows a behavior which can be approximated by a bi-linear curve with decreasing slope, the discontinuity occuring between 1.6 and 1.8 kbar. In the second portion of the curve, the computed bulk modulus derivative is 22.1. We believe that this value indicates the presence of voids which are closing under pressure. A regression analysis of the data shows that a $P^{1/2}$ equation appears to give the best fit. The resulting empirical equation for the bulk modulus derivative predicts values which are less than 6.0 at pressures in excess of 30 kbar.

APPENDIX A:

Orientation Dependence of Wave Speeds in Pyrophyllite

The results of our shear wave measurements indicated that our material was elastically anisotropic. In an effort to determine what the elastic anisotropy is, we made additional wave speed measurements on specimens of unprecompressed pyrophyllite cut at various orientations to the discs described in Section II. To specify a rectangular coordinate system in the original pyrophyllite block, we choose the axis parallel to the axis of the discs to be the x_3 axis. The x_1 and x_2 axes are perpendicular to the x_3 axis and to each other. Plane-parallel specimens of approximately 0.5 cm thickness were cut normal to each of the three axes.

The results of the wave speed measurements on each of the three specimens is listed in Table A.I. The results clearly show that the wave speed varies significantly with propagation direction. Furthermore, two distinct shear waves are observed in all three propagation directions. The shear waves sent in the x_1 - direction exhibit their maximum responses in directions which are approximately 45° to the x_2 and x_3 directions.

We attempted to determine from these measurements what matrix of elastic moduli would best describe the anistropic characteristics of the wave propagation in our specimens. Because the longitudinal wave speeds in the x_1 , x_2 and x_3 directions differ markedly, we conclude that the modulus matrix does not possess a cubic symmetry.

By assuming the pyrophyllite to be transversely isotropic, we were able to determine the non-linear algebraic equations which specify the wave speed of the longitudinal or shear wave in terms of its propagation direction cosines and the elastic moduli. Substituting the measured wave speed data into these equations and knowing the geometric relationships between the various directions of wave propagation, we can determine the five elastic constants of our material

as well as the orientations of the specimens on which the wave speed measurements were made. We used a digital computer and Newton's Method to search for the roots of our equations. Unfortunately, the results never converged to meaningful values for the elastic constants or the direction cosines. This may be a consequence of the properties of the root-searching method employed or it may indicate that the data were not obtained from an elastically transversely isotropic material. Extensions of the procedure to higher elastic anisotropies were not made because it is clear that the computations become even more untractable.

TABLE A.I

Wave Speeds ± 0.010 (cm/μsec)

Propagation Direction	Particle Displacement x_1	x_2		Direction x_3
x_1	0.306	0.233	45°	0.233
		0.215	to x_2-x_3	0.215
x_2	0.231	0.403		0.256
x_3	0.218	0.250		0.345

APPENDIX B

Because we were unsuccessful in determining the elastic anisotropy of our material from the wave speed measurements, it was impossible to provide a method by which the adiabatic bulk modulus could be specified from these measurements. As an alternative, we attempted to produce an elastically isotropic sample of pyrophyllite.

We produced a fine pyrophyllite powder (finer than 100 mesh) from the original bulk material by using a rock crusher. Compacting this in a wet-bag technique with an isostatic compaction pressure of 8 kbar, we obtained a "green" compact of pyrophyllite. Its strength was sufficient to permit the machining of several disc-like specimens of various orientations from the compact.

The specimen's density was determined with the immersion technique which was described previously. The measured density was 2.576 ± 0.002 g/cm^3 which represents 94.1% of the density of the pyrophyllite specimens which had been precompressed 40 kbars. From the wave speed measurements in various directions we found the longitudinal wave to travel at 0.361 ± 0.012 cm/μsec and the existence of one shear wave, travelling at 0.276 ± 0.010 cm/μsec, indicating that the material was elastically isotropic.

We calculate from these data an effective longitudinal modulus ($\lambda + 2\mu$) of 335.7 kbar and an effective shear modulus (μ) of 196.3 kbar. We applied the law of mixtures to the pyrophyllite-void specimen to determine the longitudinal modulus of a specimen if it consisted solely of pyrophyllite and its density was the same as that of the 40 kbar precompressed specimens. The adiabatic bulk modulus of such a material is calculated to be 96.1 kbar.

TABLE I

Modulus	C(kbar)	$0 \leq P \leq 1.6$ kbar		$1.8 \leq P \leq 3.0$ kbar	
		$\frac{dC^S}{dP}$	$\frac{1}{C_o}\frac{dC^S}{dP}(\text{kbar}^{-1})$	$\frac{dC^S}{dP}$	$\frac{1}{C_o}\frac{dC^S}{dP}(\text{kbar}^{-1})$
C_L^S	204. ± 7.0	40.39	0.198	36.20	0.177
C_S^S	113. ± 3.0	8.85	0.078	6.97	0.062
B^S	53. ± 10.0	28.59	0.539	22.13	0.418
E^S	198. ± 63.0	53.54	0.270	31.44	0.159

ACKNOWLEDGMENTS

This work was made possible by the support of the National Aeronautics and Space Administration. We acknowledge also the National Science Foundation through the use of the central facilities of the Materials Science Center at Cornell University.

We express our appreciation to Dr. J. P. Day for his assistance and the many fruitful discussions we have had with him. We are also grateful to Mr. V. Arnold for his careful machining of the numerous specimens and to Prof. J. Bird and Ms. M. Weathers for their petrographic expertise.

REFERENCES

[1] H. G. Drickamer and A. S. Balchan, in Modern Very High Pressure Techniques, R. H. Wentorf, Ed., (Butterworths and Co., Ltd., London, 1962) p. 37.

[2] C. C. Chao and A. L. Ruoff, Rev. Sci. Instr., 41, 720 (1970).

[3] A. L. Ruoff, in Advances in Cryogenic Engineering, 18, K. D. Timmerhaus, Ed., (Plenum, New York, 1973) p. 483.

[4] W. A. Deer, R. A. Howie and J. Zussman, Rock-Forming Minerals, Vol. III (Longman, London, 1971) p. 115.

[5] E. B. Dana, A Textbook of Mineralogy, (Fourth Edition), (John Wiley and Sons, New York, 1932) p. 683.

[6] S. P. Clark, Jr., Ed., Handbook of Physical Constants, (Rev. Ed.), (Geological Society of America, New York, 1966).

[7] E. P. Papadakis, J. Acoust. Soc. Am., 42, 1045 (1967).

[8] W. Sachse, J. Comp. Matls., 8, 378, (1974).

[9] Spec. Sheet, Maryland Lava Company.

[10] A. E. Carle, Brit. J. Appl. Phys., 6, 326 (1955).

[11] M. Ghafelehbashi, Ph.D. Thesis (Cornell University, Ithaca, N. Y., 1970).

[12] A. L. Ruoff, R. Lincoln and Y. C. Chen, J. Phys. D: Appl. Phys., 6, 1295 (1973).

[13] F. Birch, J. Geophys. Res., 65, 1083 (1960).

[14] F. Birch, J. Geophys. Res., 66, 2199 (1961).

[15] D. Nelson (private communication).

[16] A. Simmons and H. Wang, Single Crystal Elastic Constants and Calculated Aggregate Properties (Second Edition), (MIT Press, Cambridge, Mass., 1971).

[17] F. P. Bundy (private communication).

FIGURE CAPTIONS

Figure 1. Thin-section micrograph of Pyrophyllite.

Figure 2. Relation between the room-pressure longitudinal and the shear wave speeds (2MHZ) as a function of pre-compression pressure of pyrophyllite. Also shown (-□-) is the change in volume ratio V/V_0 as a function of the pre-compression pressure.

Figure 3. Densification of three specimens of pyrophyllite as measured by the room pressure volume ratio V/V_0 resulting from a cyclic, increasing hydrostatic pressure. Also shown is the data of Figure 2 in the range to 10 kbar.

Figure 4. Change of longitudinal and shear (fast) moduli as a function of pressure, measured during loading and unloading.

Figure 5. Linear, exponential, parabolic and general power regression analysis of the data in Figure 4.

Figure 6. Extrapolation of the analysis of Figure 5 to higher pressures.

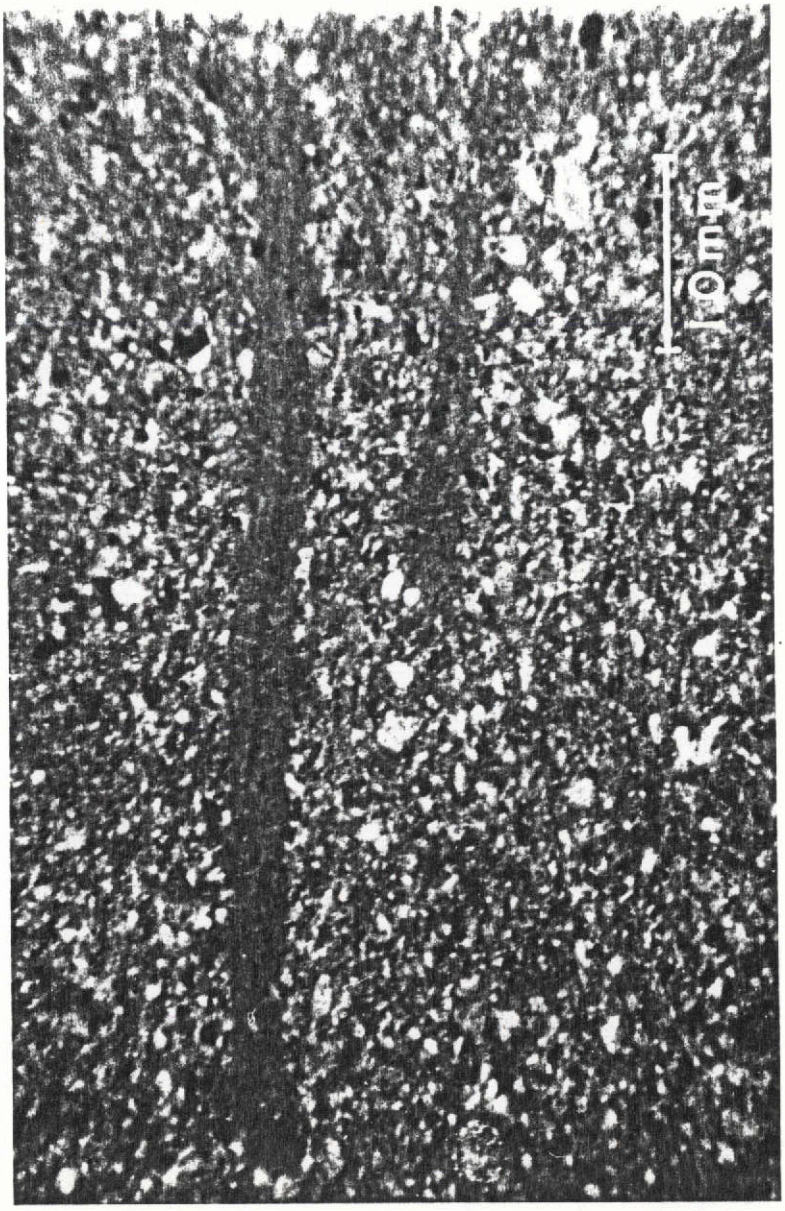

Figure 1.

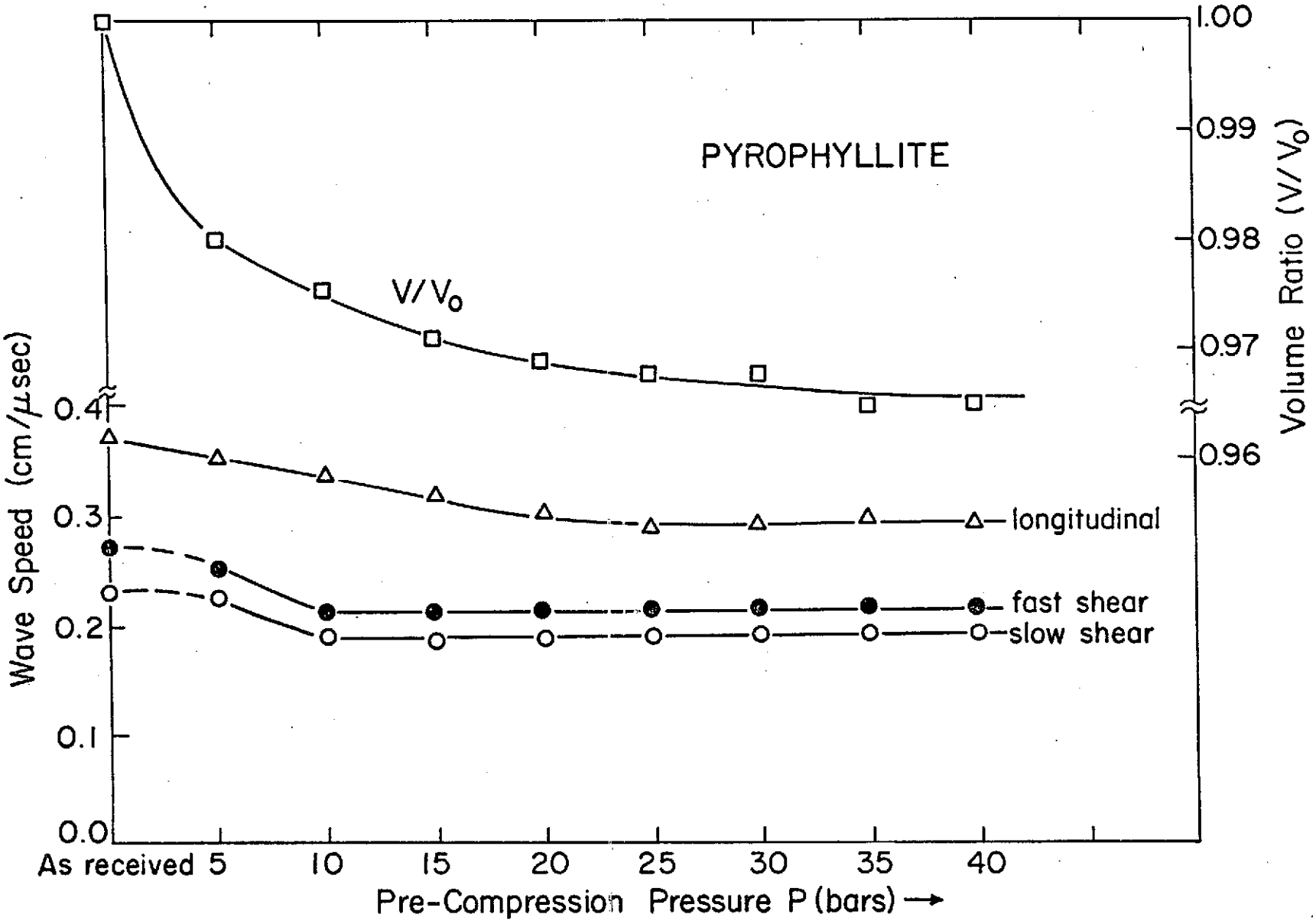
PYROPHYLLITE
V/V₀
longitudinal
fast shear
slow shear
Wave Speed (cm/μsec)
Volume Ratio (V/V₀)
1.00
0.99
0.98
0.97
0.96
0.4
0.3
0.2
0.1
0.0
As received
5
10
15
20
25
30
35
40
Pre-Compression Pressure P (bars) →

Figure 2.

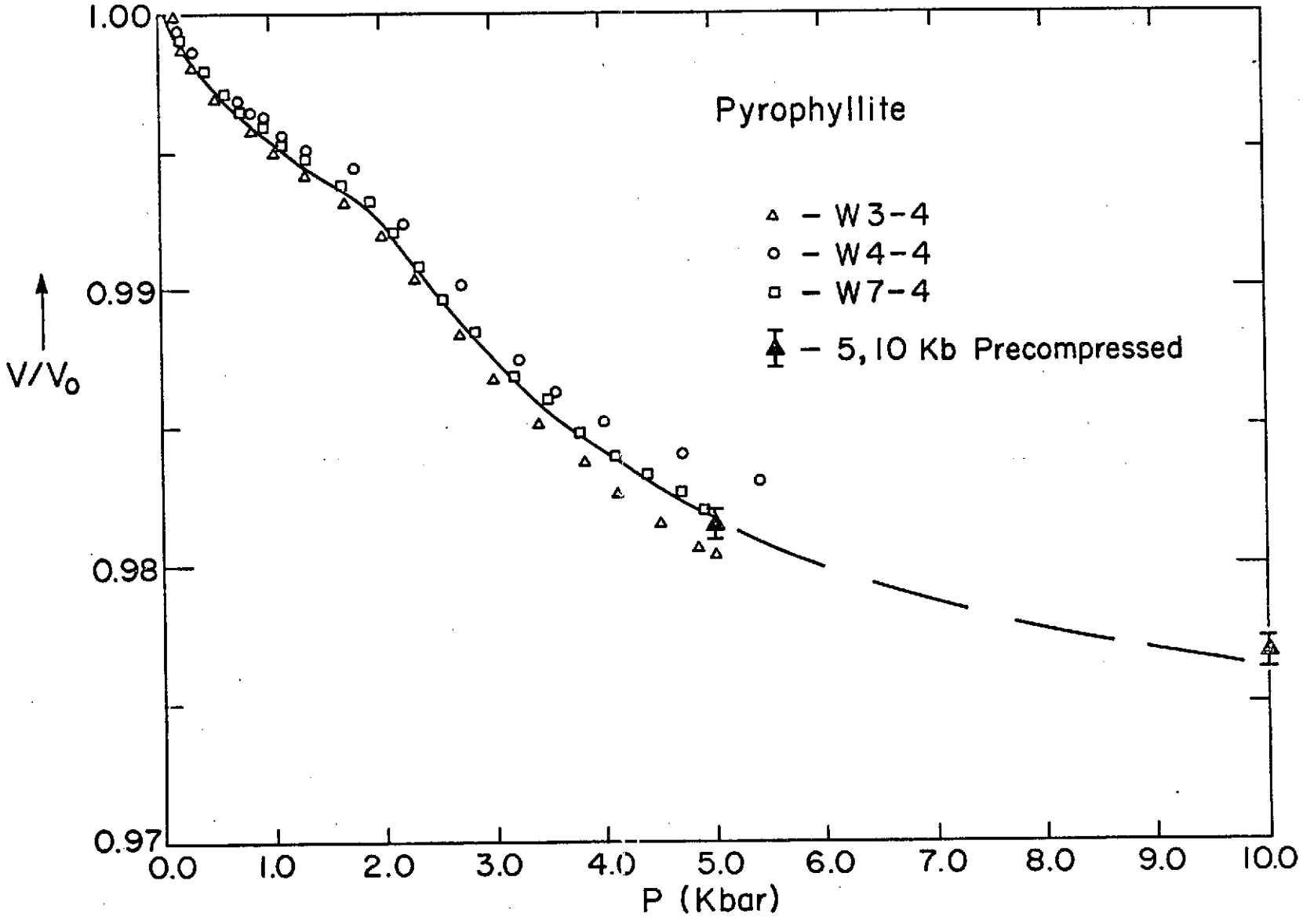
Pyrophyllite
△ – W3-4
○ – W4-4
□ – W7-4
– 5, 10 Kb Precompressed
V/V0
1.00
0.99
0.98
0.97
0.0
1.0
2.0
3.0
4.0
5.0
6.0
7.0
8.0
9.0
10.0
P (Kbar)

Figure 3.

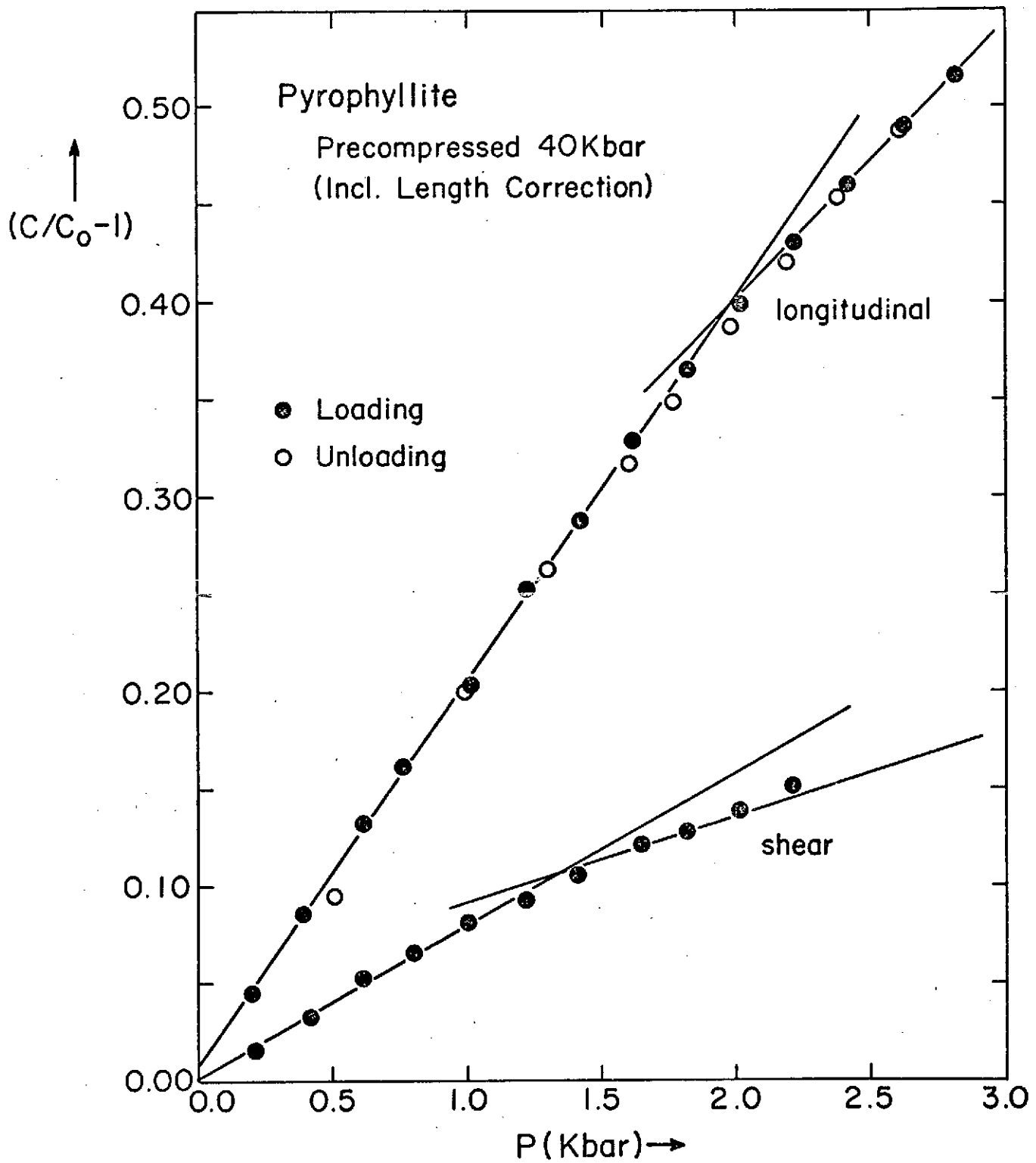
Pyrophyllite
Precompressed 40Kbar
(Incl. Length Correction)
(C/C$_o$-1)
0.50
0.40
0.30
0.20
0.10
0.00
Loading
Unloading
longitudinal
shear
0.0
0.5
1.0
1.5
2.0
2.5
3.0
P(Kbar)→

Figure 4.

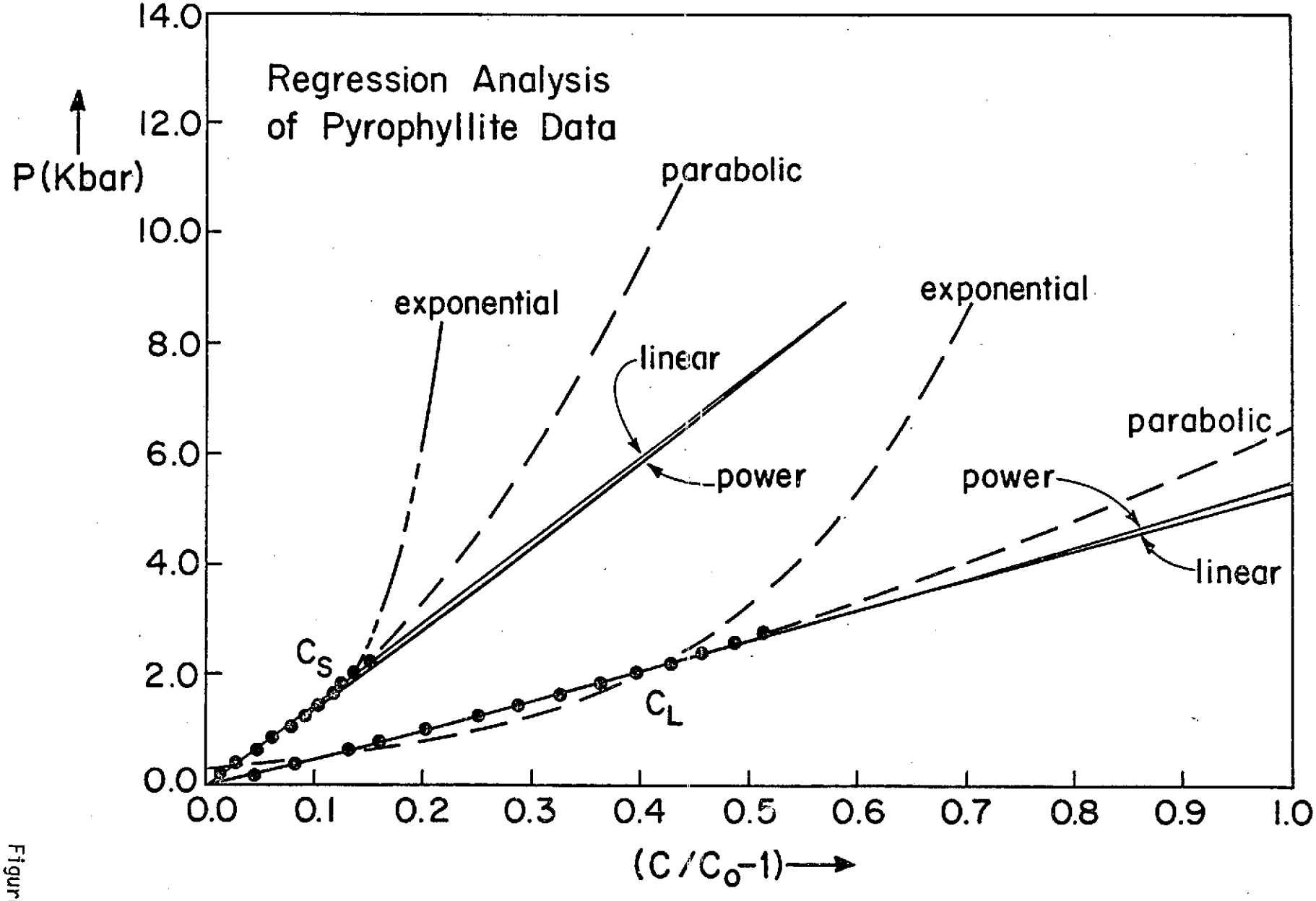
Regression Analysis
of Pyrophyllite Data
P(Kbar)
14.0
12.0
10.0
8.0
6.0
4.0
2.0
0.0
parabolic
exponential
linear
power
exponential
parabolic
power
linear
C_S
C_L
0.0
0.1
0.2
0.3
0.4
0.5
0.6
0.7
0.8
0.9
1.0
(C/C_o-1)

Figure 5.

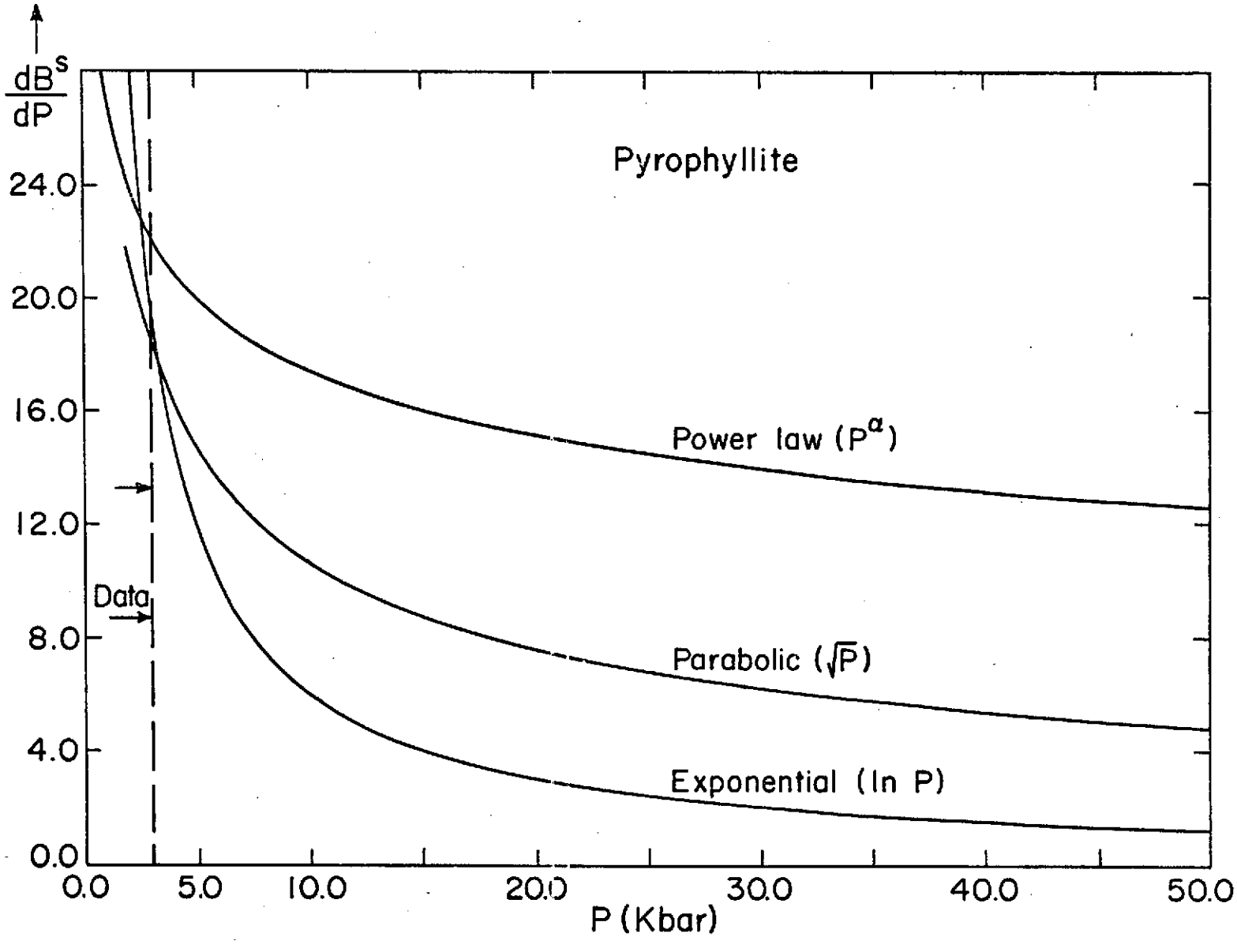
$\frac{dB^s}{dP}$
Pyrophyllite
24.0
20.0
16.0
12.0
8.0
4.0
0.0
Power law (P^{α})
Parabolic ($\sqrt{P}$)
Exponential (ln P)
Data
0.0
5.0
10.0
20.0
30.0
40.0
50.0
P (Kbar)

Figure 6.